Available online at www.sciencedirect.com
SCIENCE DIRECT®
ELSEVIER
International Journal of Solids and Structures 42 (2005) 3571–3590
INTERNATIONAL JOURNAL OF SOLIDS and STRUCTURES
www.elsevier.com/locate/ijsolstr

Multiscale homogenization of *n*-component composites with semi-elliptical random interface defects

Marcin Kamiński *

Chair of Mechanics of Materials, Technical University of Łódź, Al. Politechniki 6, 93-590 Łódź, Poland

Received 29 December 2003; received in revised form 2 November 2004
Available online 22 December 2004

Abstract

Effective elastic characteristics of periodic multicomponent composite materials with random interface defects are studied in the paper. The defects are assumed to be semi-elliptical and lying with major semi axes along the interfaces, where minor and major semi-axes as well as the defects number are given as input random variables. The homogenization approach has a multiscale character—some algebraic approximation is used first to calculate effective elastic parameters of the interphase including all defects located at the same interface. Equations for interphase random elastic parameters are obtained using MAPLE symbolic mathematics in conjunction with probabilistic generalized perturbation method. A different homogenization method is applied at the micro scale, where the cell problem is solved numerically using the Finite Element Method (FEM) program. Since the composites considered exhibit random variations of both elastic properties and the interface defects, the overall homogenized characteristics must be obtained as random quantities, which is realized on the micro scale by the Monte-Carlo simulation. The proposed interface defects model obeys the porosity effects resulting from the nature of some matrices in engineering composites as well as the interface cracks appearing as a result of composites ageing during static or fatigue fracture.

Keywords: Homogenization method; Interface defects; Random composites; Monte-Carlo simulation; Stochastic perturbation method

1. Introduction

Interface phenomena in composite materials initiating and progressing between their components can be decisive for their strength, fatigue resistance and, especially, effective mechanical properties of a composite

* Tel./fax: +48 42 6313551.
E-mail address: marcin@kmm-lx.p.lodz.pl
URL: marcinka@p.lodz.pl/pracownicy/Marcin_kaminski/index.html.

0020-7683/$ - see front matter © 2004 Elsevier Ltd. All rights reserved.
doi:10.1016/j.ijsolstr.2004.11.001

(Brandt, 1995; Mital et al., 1993; Schellekens and de Borst, 1994). According to numerous physical mechanisms like natural porosity of some materials used as matrices, cavitation erosion (Hammond et al., 1993), local shape variations of the reinforcement, initial thermal stresses (Golansky et al., 1997) resulting from manufacturing processes as well as static or fatigue micro cracks, the interface should be treated as random. Since experimental verification returns elastic properties, yield stresses etc. for composite components in statistical form, then the homogenization method should reflect this randomness. The first probabilistic models in homogenization (Ghosh et al., 1995; Jeulin and Ostoja-Starzewski, 2001; Sab, 1992) were primarily developed for heterogeneous materials and/or structures, where spatial distribution of the components is treated as random variable or field. It usually led to some algebraic approximation for effective tensor with, however, a deterministic form. Probabilistic methods development was connected with numerical techniques emerging in stochastic mechanics, where the Monte-Carlo simulation, being the oldest computational approach, played a crucial role, cf. (Cruz and Patera, 1995; Hurtado and Barbat, 1998).

The first formulation for a random composite with random interface defects was given by the stochastic perturbation-based finite element method (SFEM). Random geometry was modeled as a deterministic one and the semi-elliptical defects were homogenized in the interphase region; an alternative approach based on the interface finite elements is presented by (Schellekens and de Borst, 1994), whereas a contact finite element study can be based on the analysis included in (Zavarise et al., 1992). The random composite so defined with homogenized interphases is homogenized once more on the micro scale level using the effective moduli method and the Monte-Carlo simulation technique. Analogous deterministic micro-macro homogenization methods for composites with some defects were summarized in (Golansky et al., 1997; Lené and Leguillon, 1982). The proposed formulation forms a two-level mathematical model; it makes it possible to obtain some probabilistic characterization of the interphase effective elastic properties and, on the second level, the global homogenization of the entire Representative Volume Element (RVE). This is an essential extension of the model introduced by (Kamiński, 1995; Kamiński and Kleiber, 2000), where effective parameters of the interphase were overestimated because of the spatial averaging method applied at the interface level. Thanks to the new formulation, the final results are believed to be more accurate than the one-step averaging (or homogenization) of the entire RVE. Combined symbolic-FEM computational strategy eliminates the deficiencies of lower order perturbation techniques, offers better opportunities for composites optimization (Kalamkarov and Kolpakov, 1997; Pedersen, 1993) and visualization of homogenized characteristics for an interphase. Further engineering applications can be found in superconducting structures modeling (Kamiński and Schrefler, 2000) as well as in analysis of concrete plates reinforced with periodically distributed steel reinforcement.

2. Mathematical model

2.1. Random periodic composite

Let us consider a periodic multicomponent composite in the unstressed and undeformed plane strain state. The section of this composite structure $Y \subset \Re^2$ in the plane $x_3 = 0$, orthogonal to its longitudinal direction, where all the components are distributed in parallel, is shown in Figs. 1, 2 in the macro- and micro-scale, respectively. Let the periodic cell Ω of Y be rectangular and let the geometric dimensions of Ω be related to the corresponding dimensions of Y by a small parameter $\zeta > 0$. As is illustrated in Fig. 2, the components can show some porosity effects and some interface defects can appear in the RVE.

Let us adopt the following assumptions:

(i) elastic properties of a composite (defined on Ω) are truncated Gaussian random variables with specified and bounded first two probabilistic moments;

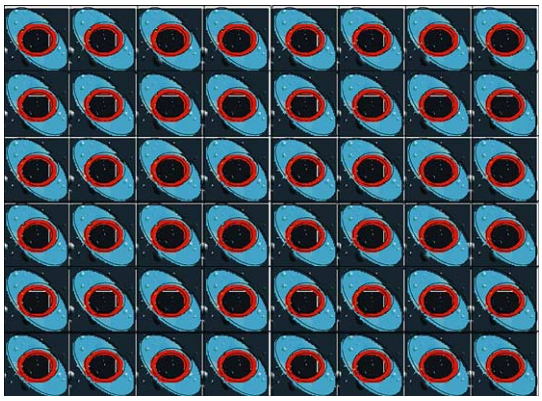

Fig. 1. Periodic composite structure Y.

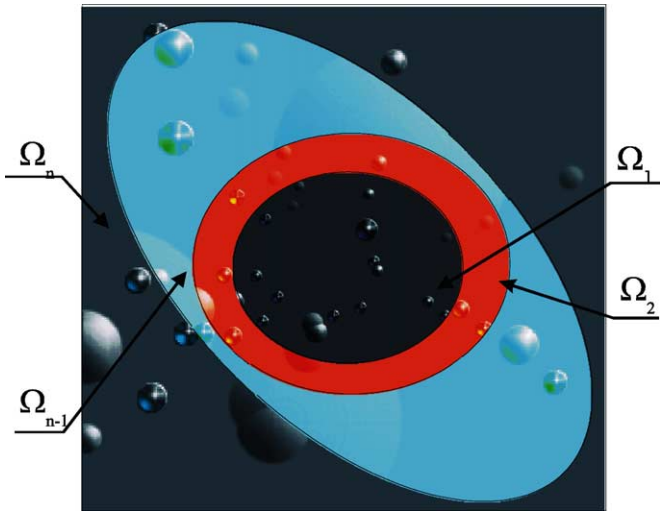

Fig. 2. The RVE of composite structure in the micro-scale.

(ii) Y is periodic in the random sense if there exists such a homothetic transformation of Ω that covers the whole Y.

Let further Ω contain n coherent regions, where $n \in N$, $n < \infty$ satisfy the following conditions:

$$\Omega = \bigcup_{r=1}^{n} \Omega_r \cup \bigcup_{r=2}^{n} \Gamma_{(r-1,r)}, \tag{1}$$

$$\Omega_r \cap \Omega_s = \varnothing, \quad \text{for } r \neq s, \ \ 1 \leqslant r, \ \ s \leqslant n, \tag{2}$$

where $\Gamma_{(r-1,r)}$ is a bounded and sufficiently regular contour being a boundary between the regions Ω_{r-1} and Ω_r. Let us consider such a class of periodicity cells Ω that for every r an interior of contour $\Gamma_{(r-2,r-1)}$ is contained in the interior of contour $\Gamma_{(r-1,r)}$ and these contours are disjoint. Moreover, let us assume a form of microcontact to exist on the boundary $\Gamma_{(r-1,r)}$ with some random material defects (or discontinuities)

occurring on this boundary. Let D_r be the total area of the discontinuities belonging to Ω_r both on boundaries $\Gamma_{(r-1,r)}$ (denoted as D'_r) and $\Gamma_{(r,r+1)}$(denoted as D''_r), respectively. Let C_r be a continuum region belonging to Ω_r. Next, let C_r be, for every $1 \leqslant r \leqslant n$, a linear-elastic transversely isotropic domain, in which the Young modulus is a truncated Gaussian random variable with specified expected values

$$E[e(\omega)] = E\lfloor e_r(\omega)\rfloor, \quad \text{for } r = 1,2,\ldots,n; \ \ \mathbf{x} \in \Omega_r, \tag{3}$$

and variances

$$\mathrm{Var}(e(\omega)) = \mathrm{Var}(e_r(\omega)), \quad \text{for } r = 1,2,\ldots,n; \ \ \mathbf{x} \in \Omega_r \tag{4}$$

ω is a random event belonging to the space of elementary events S with non-negative and bounded real values only. Furthermore, it is assumed that the Young moduli in different regions Ω_r are uncorrelated random variables

$$\mathrm{Cov}(e_r(\omega), e_s(\omega)) = 0, \quad \text{for } r,s = 1,2,\ldots,n; \ \ r \neq s. \tag{5}$$

Let us note that the Young moduli are taken as random variables to compare the influence of their randomness against the influence of randomness of interface defects parameters on the expected values and variances of the effective elasticity tensor; the Poisson ratio is assumed now to be a deterministic function, so that

$$v(\mathbf{x}) = v_r; \quad \mathbf{x} \in \Omega_r. \tag{6}$$

Then, the random elasticity tensor field $C_{ijkl}(\mathbf{x};\omega)$ is defined as follows

$$C_{ijkl}(\mathbf{x};\omega) = e(\mathbf{x};\omega)\left\{\delta_{ij}\delta_{kl}\frac{v(\mathbf{x})}{(1+v(\mathbf{x}))(1-2v(\mathbf{x}))} + (\delta_{ik}\delta_{jl}+\delta_{il}\delta_{jk})\frac{1}{2(1+v(\mathbf{x}))}\right\}, \tag{7}$$

where $i,j,k,l = 1,2$.

All the elastic characteristics are equal to 0 for any $\mathbf{x} \in D_r$, $1 \leqslant r \leqslant n$. Because of the linear dependence between the elasticity tensor components and the Young modulus (cf. Eq. (7)), these components have the truncated Gaussian distributions as well. Therefore their moments can be derived uniquely from the first two probabilistic moments of the relevant Young modulus. Using a definition of the expected value and variance of the random variable and denoting

$$A_{ijkl}(\mathbf{x}) = \delta_{ij}\delta_{kl}\frac{v(\mathbf{x})}{(1+v(\mathbf{x}))(1-2v(\mathbf{x}))} + (\delta_{ik}\delta_{jl}+\delta_{il}\delta_{jk})\frac{1}{2(1+v(\mathbf{x}))}, \quad \text{for } i,j,k,l = 1,2, \tag{8}$$

there holds

$$E(C_{ijkl}(\mathbf{x};\omega)) = A_{ijkl}(\mathbf{x}) \cdot E(e(\mathbf{x};\omega)) \tag{9}$$

and

$$\mathrm{Cov}\big(C_{ijkl}(e_r(\omega)); C_{mopq}(e_s(\omega))\big) = A_{ijkl}(\mathbf{x}) \cdot A_{mopq}(\mathbf{x}) \cdot \mathrm{Cov}(e_r(\omega); e_s(\omega)), \tag{10}$$

where $i,j,k,l,m,o,p,q = 1,2$ and $r,s = 1,2,\ldots,n$.

2.2. Geometry of random interface defects

Let us consider a microcontact surface between Ω_{r-1} and Ω_r on the interface $\Gamma_{(r-1,r)}$ (cf. Fig. 3). Let us assume an approximation of material discontinuities occurring on this boundary by random bubbles with semi-elliptical shapes, where smaller and greater semi-axes a, b as well as the total number of these defects n are random variables defined using expected values and their variances. The bubbles major semi-axes coincide with the boundary $\Gamma_{(r-1,r)}$; its curvatures is neglected and the bubbles are assumed not to overlap. The parameters of the bubbles are assumed to have all positive values only. Further, let for every Ω_r the

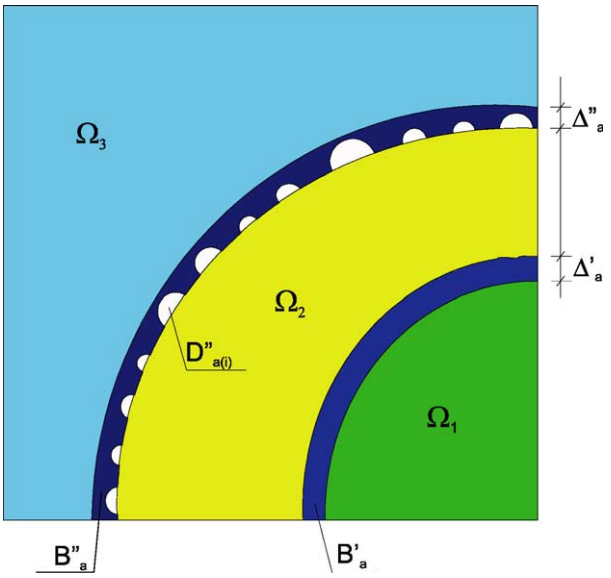

Fig. 3. Interface micro-geometry in multicomponent composite.

expected values and variances of the defect semi-axes and their total number be given. Let us note that such an approximation of the interface defects is quite close to the structural defects idealization well-known from fracture mechanics.

In order to formulate a homogenization method for the stochastic interface defects, the subsets $B'_r \subset \Omega_r$ and $B''_r \subset \Omega_r$ are introduced, such that with a probability equal to 1 there holds $D'_r \subset B'_r$ and $D''_r \subset B''_r$. For this purpose, for $r = 1, 2, \ldots, n$ the random variables $\Delta'_r(\omega)$ and $\Delta''_r(\omega)$ are defined as the upper bounds on norms of the vectors normal to the interfaces $\Gamma_{(r-1,r)}$ and $\Gamma_{(r,r+1)}$

$$\Delta'_r(\omega) = \sup_{D'_r}\{|\,\vec{AE}\,|: A \in \Gamma_{(r-1,r)}; E \in D'_r; \vec{AE} \perp \Gamma_{(r-1,r)}\}, \tag{11}$$

$$\Delta''_r(\omega) = \sup_{D''_r}\{|\,\vec{AE}\,|: A \in \Gamma_{(r,r+1)}; E \in D''_r; \vec{AE} \perp \Gamma_{(r,r+1)}\}. \tag{12}$$

The vectors $\vec{AE}$ are defined on the boundaries $\Gamma_{(r-1,r)}$, $\Gamma_{(r,r+1)}$ and the boundaries of random interface defects belonging to D_a. To introduce a description for B'_r and B''_r let us consider the upper bounds for probabilistic distributions of $\Delta'_r(\omega)$ and $\Delta''_r(\omega)$ as

$$\Delta'_r = E[\Delta'_r(\omega)] + 3 \cdot \sqrt{\mathrm{Var}(\Delta'_r(\omega))}, \tag{13}$$

$$\Delta''_r = E[\Delta''_r(\omega)] + 3 \cdot \sqrt{\mathrm{Var}(\Delta''_r(\omega))}. \tag{14}$$

Thus B'_r and B''_r can be expressed in the following form:

$$B'_r = \{P(\mathbf{x}) \in \Omega_r; d(P, \Gamma_{(r-1,r)}) \leqslant \Delta'_r\}, \tag{15}$$

$$B''_r = \{P(\mathbf{x}) \in \Omega_r; d(P, \Gamma_{(r,r+1)}) \leqslant \Delta''_r\}, \tag{16}$$

where $i = 1, 2$, $r = 1, 2, \ldots, n$ and $d(P, \Gamma)$ denotes the distance from point P to contour Γ. Finally, the micro-contact problem of the composite with random interface defects is modelled using an equivalent random

elastostatics problem for the composite with perfect interfaces, where elastic constants $e(\mathbf{x};\omega)$ and $\nu(\mathbf{x})$ of the continuous interphases are obtained by homogenization of the defects with the remaining material into the regions B_r, $r = 1,2,\ldots,n$.

2.3. Determination of the effective properties for the interphase

The constitutive interphase model provided here is based on the observation that the isotropic effective elastic properties of the interphase are identical to those of a medium with randomly distributed elliptical holes. Deterministic formulas derived for this model before (Jasiuk et al., 1994; Tsukrov and Kachanov, 2000) are extended now, using a probabilistic perturbation technique to determine the first two moments for interphase effective parameters. It should be underlined that the tensor quantity $\boldsymbol{\beta}$ introduces into the model both circular and elliptical voids as well as the interfacial cracks, and that is why the interphase model obeys all these phenomena at the interface.

The homogenized properties of the interphase between fiber and matrix are calculated as for an isotropic linear elastic medium containing elliptical structural defects. The approach is based on the results obtained for a single elliptical cavity. Let us represent the total strain in a solid subjected to the applied stress $\boldsymbol{\sigma}$ by the following sum:

$$\boldsymbol{\varepsilon} = \mathbf{c}^0\boldsymbol{\sigma} + \Delta\boldsymbol{\varepsilon}, \tag{17}$$

where the tensor $\mathbf{c}^0$ is a compliance tensor of the matrix without defect. The additional strain due to the introduction of a defect is equal to

$$\Delta\boldsymbol{\varepsilon} = -\frac{1}{2\mid\Omega\mid}\int_{\partial\Omega}(\mathbf{un}+\mathbf{nu})\,\mathrm{d}(\partial\Omega) \tag{18}$$

with $\mathbf{u}$ and $\mathbf{n}$ denoting displacements of the defect boundary $\partial\Omega$ and the unit vector normal to this boundary (directed into the defect), Ω is the total (including a defect) reference area of the tensioned specimen. The elastic potential (complementary energy density) $f(\boldsymbol{\sigma})$ can be expressed as

$$f(\boldsymbol{\sigma}) = \frac{1}{2}\boldsymbol{\sigma}\mathbf{c}^0\boldsymbol{\sigma} + \frac{1}{2}\boldsymbol{\sigma}\mathbf{H}\boldsymbol{\sigma} = f_0(\boldsymbol{\sigma}) + \Delta f(\boldsymbol{\sigma}), \tag{19}$$

where

$$f_0(\boldsymbol{\sigma}) = \frac{1}{2E_0}\left((1+\nu_0)\mathrm{tr}(\boldsymbol{\sigma}\boldsymbol{\sigma}) - \nu_0(\mathrm{tr}(\boldsymbol{\sigma}))^2\right) \tag{20}$$

and $\Delta f(\boldsymbol{\sigma})$ is the change in elastic potential due to the defect presence. For a single elliptical hole in a homogeneous and isotropic solid under uniaxial loading P inclined at the angle α, it yields

$$\begin{cases} \Delta\varepsilon_{11} = \dfrac{P\pi b}{AE_0}(b + (a+b)\cos 2\alpha), \\ \Delta\varepsilon_{22} = \dfrac{P\pi a}{AE_0}(a - (a+b)\cos 2\alpha), \\ \Delta\varepsilon_{12} = \dfrac{P\pi}{2AE_0}(a+b)^2\sin 2\alpha \end{cases} \tag{21}$$

when the notation introduced is consistent with Fig. 4.

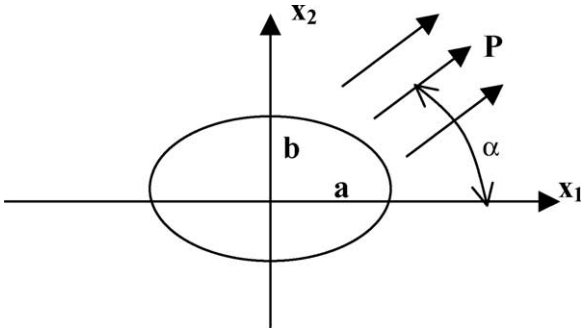

Fig. 4. Structural defect under a general uniaxial loading P.

The defect compliance tensor can be found as (Tsukrov and Kachanov, 2000)

$$\mathbf{H} = \frac{\pi}{AE_0}\left[a(2a+b)\mathbf{nnnn} + b(2b+a)\mathbf{mmmm} + \frac{1}{2}(a+b)^2(\mathbf{mn}+\mathbf{nm})(\mathbf{mn}+\mathbf{nm}) - ab(\mathbf{mmnn}+\mathbf{nnmm})\right], \tag{22}$$

where $\mathbf{m},\mathbf{n}$ are unit normals to the axes $2b$ and $2a$ of the ellipse (the axis x_1 is tangent to the interface in our model). The first two terms characterize the normal compliances of the defect in the $\mathbf{m}$ and $\mathbf{n}$ directions, the third term—the shear compliance and the fourth term corresponds to the Poisson ratio effect. After some algebra one can get that

$$\Delta f(\boldsymbol{\sigma}) = \boldsymbol{\sigma}\sum_k \mathbf{H}^{(k)}\boldsymbol{\sigma} = \frac{1}{2E_0}\left(p[4\mathrm{tr}(\boldsymbol{\sigma}\boldsymbol{\sigma}) - (\mathrm{tr}(\boldsymbol{\sigma}))^2] + 2\boldsymbol{\sigma}\boldsymbol{\sigma}(\boldsymbol{\beta} - p\mathbf{I})\right) \tag{23}$$

with

$$p = \frac{1}{A}\sum_k (ab)^{(k)} \tag{24}$$

being a porosity parameter and

$$\boldsymbol{\beta} = \frac{\pi}{A}\sum_k (a^2\mathbf{nn} + b^2\mathbf{mm})^{(k)} \tag{25}$$

is the second rank defect density tensor. Its linear invariant is equal to

$$\mathrm{tr}(\boldsymbol{\beta}) = \frac{1}{A}\sum_k (a^2+b^2)^{(k)} \tag{26}$$

and it characterizes the influence of the defects in the overall compressibility of the weakened material. For cracks the term $\left(\frac{1}{\pi}\right)\beta$ reduces to the plane crack density tensor $\boldsymbol{\alpha} = \frac{1}{A}\sum_k (a^2\mathbf{nn})^{(k)}$, while for circular holes $\boldsymbol{\beta} = p\mathbf{I}$ and Δf becomes a potential of the isotropic body being proportional to the porosity parameter. Therefore, the effective moduli are equal to

$$\frac{e^{(\mathrm{eff})}_{\{1,2\}}}{e_m} = (1 + p + 2\{\beta_{11}, \beta_{22}\})^{-1} \tag{27}$$

as well as

$$\left\{ v_{12}^{(\mathrm{eff})}, v_{21}^{(\mathrm{eff})} \right\} = \frac{v_m + p}{1 + p + 2\{\beta_{11}, \beta_{22}\}}. \tag{28}$$

For randomly oriented defects isotropic effective properties are obtained and there holds in this case

$$\beta_{11} = p + \frac{q}{2}; \tag{29}$$

then

$$e_i^{(\mathrm{eff})} = \frac{e_m}{1 + p + 2\beta_{11}} \tag{30}$$

as well as

$$v_i^{(\mathrm{eff})} = \frac{v_m + p}{1 + p + 2\beta_{11}}. \tag{31}$$

It should be emphasized that these moduli cannot be expressed in terms of porosity alone: the shape factor like eccentricity parameter q is also necessary.

$$q = \frac{\pi}{A} \sum (a - b)^2 = \frac{n\pi}{2\Omega_i} (a - b)^2. \tag{32}$$

If this factor is ignored, then the homogenized porosity is overestimated, which is the subject of further computational studies. Further, it yields

$$p = \frac{n \frac{\pi ab}{2}}{\pi\{(R + E[a] + 3\sigma(a))^2 - R^2\}} = \frac{nab}{2\{(R + E[a] + 3\sigma(a))^2 - R^2\}}. \tag{33}$$

Because the denominator consists of some deterministic function and n, a, b are introduced as uncorrelated random variables, then probabilistic moments of porosity parameter can be derived explicitly. Using basic definitions and properties of random variables (Feller, 1965) one can demonstrate that

$$E[p] = \frac{E[n]E[a]E[b]}{2\{(R + E[a] + 3\sigma(a))^2 - R^2\}} \tag{34}$$

as well as

$$\begin{aligned} \mathrm{Var}(p) = {} & \frac{1}{4\left\{ (R + E[a] + 3\sigma(a))^2 - R^2 \right\}^2} \{E^2[n]\mathrm{Var}(a)\mathrm{Var}(b) + \mathrm{Var}(n)E^2[a]\mathrm{Var}(b) + \mathrm{Var}(n)\mathrm{Var}(a)E^2[b] \\ & + E^2[n]E^2[a]\mathrm{Var}(b) + \mathrm{Var}(n)E^2[a]E^2[b] + E^2[n]\mathrm{Var}(a)E^2[b] + \mathrm{Var}(n)\mathrm{Var}(a)\mathrm{Var}(b)\}. \end{aligned} \tag{35}$$

Since Eqs. (30) and (31) consists of an inverse of Gaussian variables, the integrals defining expected values as well as higher order moments may not converge in the general case. Therefore probabilistic perturbation methodology is proposed to calculate these moments. It is based on an expansion via Taylor series about the spatial expectations using a small parameter $\varepsilon > 0$ and, for some random output, the following expression is employed:

$$f = f^0 + \varepsilon f^{,b} \Delta b + \frac{1}{2} \varepsilon^2 f^{,bb} \Delta b \Delta b + \cdots + \frac{1}{n!} \varepsilon^n \frac{\partial^n f}{\partial x^n} (\Delta b)^n, \tag{36}$$

where b stands for the random input, Δb denotes the variation of this variable around its expected value. The accuracy of this expansion depends much on the perturbation order. In a general case, the variable b

can be replaced with the random vector including defects semi-axes and the total number in the analyzed problem. Following this expression, the expected value and the variance of the resulting function 'f' can be obtained as

$$\begin{aligned} E[f(t,b);b] &= 1 \times f^{0}(t,b) + \frac{1}{2} \times f^{,bb}(t,b) \times \mathrm{Var}(b) + \frac{1}{4!} \times f^{,bbbb}(t,b) \times \mu_4(b) \\ &\quad + \frac{1}{6!} \times f^{,bbbbbb}(t,b) \times \mu_6(b) + \cdots \\ &= f^{0}(t,b) + \frac{1}{2} f^{(2)}(t,b) + \frac{1}{4!} f^{(4)}(t,b) + \frac{1}{6!} f^{(6)}(t,b) + \cdots \end{aligned} \tag{37}$$

and, furthermore

$$\begin{aligned} \mathrm{Var}(f) &= \mathrm{Var}(b) \times f^{,b} f^{,b} + \mu_4(b) \times \left(\frac{1}{4} f^{,bb} f^{,bb} + \frac{2}{3!} f^{,b} f^{,bbb} \right) \\ &\quad + \mu_6(b) \times \left(\left(\frac{1}{3!} \right)^2 f^{,bbb} f^{,bbb} + \frac{1}{4!} f^{,bbbb} f^{,bb} + \frac{2}{5!} f^{,bbbbb} f^{,b} \right) + \cdots, \end{aligned} \tag{38}$$

where $\mu_k(b)$ is kth order central probabilistic moment of the variable b. The perturbation parameter is adopted as $\varepsilon = 1$ in Eqs. (37) and (38) and only the first few perturbations are included, especially in the last relation. As it can be seen in these equations, the symbolic approach perfectly reflects the needs of higher order perturbation approaches, where automatic differentiation can be efficiently used in conjunction with higher order statistics for the relevant products of random functions; a perturbation parameter with increasing powers can be inserted directly in the Taylor series expansion, too. This opportunity is realized in numerical experiments to compute symbolically up to the 10th order expression for interphase homogenized parameters to eliminate the deficiencies of the perturbation technique itself. Finally, let us emphasize that the interphase model can be further extended to more general defects shapes (Leo and Hu, 1995), anisotropic effective constitutive law, interacting interface defects, progressing debonding process of the fiber from surrounding matrix and so forth (Jasiuk et al., 1994; Litewka, 1985; Tsukrov and Kachanov, 2000).

2.4. Homogenization of a composite structure with n-components in the RVE

A homogenization procedure for multicomponent materials consists generally in determining the so-called effective properties that characterize the homogeneous medium equivalent in a desired physical sense to the original medium. The criteria of equivalence can be generally quite different; the method presented here is based on the assumption that the strain energies stored in both media (real and homogenized) are approximately equal (in the sense of weak convergence with scaling parameter tending to 0).

There are two main reasons of significance of the homogenization for computational analysis of composite structures. The first one is that the FEM discretization of such media is very complicated and consumes a lot of computational time. Moreover, while modeling composites, engineers are interested in global macroscopic behavior rather than in the micro- or mesoscale effects.

To obtain a reliable macro model of composite behavior and to carry out the macro discretization only, the macro state functions (stress, strains and displacements) should be expressed by the use of the micro functions and a geometrical scaling parameter $\zeta > 0$ introduced in Section 2.1. First, let us introduce two coordinate systems $\mathbf{y} = (y_1, y_2, y_3)$ on the microscale of the composite and $\mathbf{x} = (x_1, x_2, x_3)$ on the macroscale. Next, let us consider any periodic state function F defined on the whole $\mathfrak{R}^2$ set and note that the function can be expressed as

$$F^{\zeta}(\mathbf{x}) = F\left(\frac{\mathbf{x}}{\zeta}\right) = F(\mathbf{y}). \tag{39}$$

This expression allows us to describe the macro functions in terms of the micro ones and vice versa. Thus, the cell problem for a linear elastic periodic structure is formulated as follows (Bensoussan et al., 1978; Sanchez-Palencia, 1980; Kalamkarov and Kolpakov, 1997; Kamiński, 1995):

$$\begin{cases} \dfrac{\partial \sigma_{ij}^{\zeta}}{\partial x_j} = 0 \\ \sigma_{ij}^{\zeta} n_j = p_i; \quad \mathbf{x} \in \partial\Omega_{\sigma} \\ u_i^{\zeta} = 0; \quad \mathbf{x} \in \partial\Omega_u \\ \sigma_{ij}^{\zeta} = C_{ijkl}^{\zeta}(\mathbf{x})\varepsilon_{kl}^{\zeta} \\ \varepsilon_{kl}^{\zeta} = \frac{1}{2}\left(u_{k,l}^{\zeta} + u_{l,k}^{\zeta}\right) \end{cases} \qquad i,j,k,l = 1,2. \tag{40}$$

Next, it is assumed that all interfaces of the composite are perfect in the microscale, which means

$$[u_i^{\zeta}] = 0, [\sigma_{ij} n_j^{\Gamma}] = 0, \tag{41}$$

where [.] denotes a jump of value of the relevant function at the interface. To solve this problem, it is assumed that ζ tends to 0. Let us consider a bilinear form $a^{\zeta}(\mathbf{u},\mathbf{v})$

$$a^{\zeta}(\mathbf{u},\mathbf{v}) = \int_{\Omega} C_{ijkl}\left(\frac{\mathbf{x}}{\zeta}\right)\varepsilon_{ij}(\mathbf{u})\varepsilon_{kl}(\mathbf{v})\,\mathrm{d}\Omega \tag{42}$$

and a linear form

$$L(\mathbf{v}) = \int_{\Omega} F_i v_i \,\mathrm{d}\Omega + \int_{\partial\Omega_{\sigma}} p_i v_i \,\mathrm{d}(\partial\Omega) \tag{43}$$

in the following Hilbert space

$$V = \left\{\mathbf{v} \mid \mathbf{v} \in \left(H^1(Y)\right)^3, \mathbf{v}|_{\partial\Omega_u} = 0\right\}, \tag{44}$$

$$\|\mathbf{v}\|^2 = \int_{\Omega} \varepsilon_{ij}(\mathbf{v})\varepsilon_{ij}(\mathbf{v})\,\mathrm{d}\Omega. \tag{45}$$

The variational statement equivalent to the equilibrium problem (40) is to find $\mathbf{u}^{\zeta} \in V$ being a solution of the following equation:

$$a^{\zeta}(\mathbf{u}^{\zeta},\mathbf{v}) = L(\mathbf{v}) \tag{46}$$

for any $\mathbf{v} \in V$. For this purpose let us define a space of periodic functions $P(\Omega) = \{\mathbf{v}, \mathbf{v} \in (H^1(\Omega))^3\}$, so that the trace of $\mathbf{v}$ is equal on the opposite sides of Ω. Let us introduce the following bilinear form for any $\mathbf{u},\mathbf{v} \in P(\Omega)$:

$$a_y(\mathbf{u},\mathbf{v}) = \int_{\Omega} C_{ijkl}(\mathbf{y})\varepsilon_{ij}(\mathbf{u})\varepsilon_{kl}(\mathbf{v})\,\mathrm{d}\Omega \tag{47}$$

and let us introduce a homogenization function $\chi_{(ij)k} \in P(\Omega)$ as a solution for the so-called local problem on a periodicity cell

$$a_y\left(\left(\chi_{(ij)k} + y_j\delta_{ki}\right)\mathbf{n}_k, \mathbf{w}\right) = 0 \tag{48}$$

for any $\mathbf{w} \in P(\Omega)$, where $\mathbf{n}_k$ is the unit coordinate vector. It can be proved that the problem has a unique solution up to the constant terms.

Assuming that

$$C_{ijkl} \in L^{\infty}(\Re^3), \tag{49}$$

$$C_{ijkl} = C_{klij} = C_{jikl}, \tag{50}$$

$$\forall \xi_{ij} = \xi_{ji}, \quad \exists C_0 > 0; \;\; C_{ijkl}\xi_{ij}\xi_{kl} \geqslant C_0 \xi_{ij}\xi_{ij}, \tag{51}$$

the effective elasticity tensor components can be found from the following theorem:

Homogenization theorem

The solution $\mathbf{u}^{\zeta}$ of problem (46) converges weakly in space V

$$\mathbf{u}^{\zeta} \to \mathbf{u} \tag{52}$$

if the tensor $C^{\zeta}_{ijkl}(\mathbf{y})$ is Ω-periodic and its components fulfill conditions (49)–(51). The solution $\mathbf{u}$ is the unique solution of the problem

$$\mathbf{u} \in V, \quad S(\mathbf{u}, \mathbf{v}) = L(\mathbf{v}) \tag{53}$$

for any $\mathbf{v} \in V$ and

$$S(\mathbf{u}, \mathbf{v}) = \int_Y S_{ijkl}\varepsilon_{ij}(\mathbf{u})\varepsilon_{kl}(\mathbf{v})\,\mathrm{d}Y, \tag{54}$$

where

$$S_{ijkl} = \frac{1}{|\,\Omega\,|} a_y\Big(\Big(\chi_{(ij)p} + y_i\delta_{pj}\Big)\mathbf{n}_p, \Big(\chi_{(kl)r} + y_l\delta_{rk}\Big)\mathbf{n}_r\Big). \tag{55}$$

To provide a solution for the n-component periodic fiber-like composite defined in Section 2.1, the local problem is considered in its differential form

$$\frac{\partial}{\partial x_j}\left(C_{ijkl}\left(\frac{\mathbf{x}}{\zeta}\right)\varepsilon_{kl}(\mathbf{u}^{\zeta})\right) + F_i = 0; \quad u_i^{\zeta} = 0 \;\text{ for } \mathbf{y} \in \partial\Omega. \tag{56}$$

Next, the following representation is introduced for the displacement field by means of parameter ζ as follows:

$$\mathbf{u}^{\zeta}(\mathbf{x}) = \sum_{m=1}^{\infty} \zeta^m u^{(m)}(\mathbf{x}, \mathbf{y}), \tag{57}$$

where any $\mathbf{u}^{(m)}(\mathbf{x}, \mathbf{y})$ is periodic in $\mathbf{y}$ with a periodicity cell Ω. Let us note that the differentiation separates the variables $\mathbf{x}$ and $\mathbf{y}$ so that

$$\varepsilon_{ij}(\mathbf{v}) = \varepsilon^x_{ij}(\mathbf{v}) + \frac{1}{\zeta}\varepsilon^y_{ij}(\mathbf{v}), \tag{58}$$

where $\varepsilon^x_{ij}(\mathbf{v})$ can be described as

$$\varepsilon^x_{ij}(\mathbf{v}) = \frac{1}{2}\left(\frac{\partial v_i}{\partial x_j} + \frac{\partial v_j}{\partial x_i}\right), \tag{59}$$

while $\varepsilon^y_{ij}(\mathbf{v})$ can be expressed in a similar form by the derivation with respect to y. Thus Eq. (56) can be rewritten in the following form:

$$\left(\zeta^{-2}L_1 + \zeta^{-1}L_2 + L_3\right) \cdot \sum_{m=1}^{\infty} \zeta^m u^{(m)}(\mathbf{x}, \mathbf{y}) + \mathbf{F} = 0, \tag{60}$$

where

$$L_1\mathbf{u} = \frac{\partial}{\partial y_i}(C_{ijkl}(\mathbf{y}))\varepsilon^y_{kl}(\mathbf{u}), \tag{61}$$

$$L_2\mathbf{u} = C_{ijkl}(\mathbf{y})\frac{\partial}{\partial x_j}(\varepsilon^y_{kl}(\mathbf{u})) + \frac{\partial}{\partial y_i}\left(C_{ijkl}(\mathbf{y})\varepsilon^x_{kl}(\mathbf{u})\right), \tag{62}$$

$$L_3\mathbf{u} = C_{ijkl}(\mathbf{y})\frac{\partial}{\partial x_j}\left(\varepsilon^x_{kl}(\mathbf{u})\right). \tag{63}$$

Next, by equating the terms with the same order of ζ to 0, an infinite sequence of equations of zeroth, first and second order relations is obtained. They can be written as

$$L_1\mathbf{u}^{(0)} = 0, \tag{64}$$

$$L_1\mathbf{u}^{(1)} + L_2\mathbf{u}^{(0)} = 0, \tag{65}$$

$$L_1\mathbf{u}^{(2)} + L_2\mathbf{u}^{(1)} + L_3\mathbf{u}^{(0)} + \mathbf{F} = 0. \tag{66}$$

Functions $\mathbf{u}^{(0)}$, $\mathbf{u}^{(1)}$ and $\mathbf{u}^{(2)}$ can be found from these equations recurrently if only $\mathbf{x}$ and $\mathbf{y}$ are independent variables. Let us also note that the equation

$$L_1\mathbf{u} + \mathbf{P} = 0 \tag{67}$$

for $\mathbf{u}$ being a Ω-periodic function has a unique solution for

$$\langle\mathbf{P}\rangle = \frac{1}{|\,\Omega\,|}\int_{\Omega}\mathbf{P}\,\mathrm{d}\mathbf{y} = 0. \tag{68}$$

Starting from the above equations, it yields

$$\mathbf{u}^{(0)}(\mathbf{x},\mathbf{y}) = \mathbf{u}(\mathbf{x}), \tag{69}$$

while Eq. (61) takes the following form:

$$L_1\mathbf{u}^{(1)}(\mathbf{x},\mathbf{y}) + \frac{\partial}{\partial y_i}(C_{ijkl}(\mathbf{y}))\varepsilon^x_{kl}\left(\mathbf{u}^{(0)}(\mathbf{x})\right) = 0. \tag{70}$$

A separation of the variables $\mathbf{x}$ and $\mathbf{y}$ leads to

$$u^{(1)}_i(\mathbf{x},\mathbf{y}) = \chi_{(kl)i}(\mathbf{y})\varepsilon^x_{kl}\left(\mathbf{u}^{(0)}\right) + u_i(\mathbf{x}). \tag{71}$$

The last two equations give the formulation for the Ω-periodic functions $\chi_{(kl)i}(\mathbf{y})$ as

$$\frac{\partial}{\partial y_i}\left(C_{ijkl}(\mathbf{y})\frac{\partial\chi_{(kl)m}(\mathbf{y})}{\partial y_m}\right) + \frac{\partial}{\partial y_i}C_{ijkl}(\mathbf{y}) = 0. \tag{72}$$

It is seen that the local problem for the homogenization function $\chi_{(kl)i}(\mathbf{y})$ reduces to the equations posed above for any region Ω_r, where $1 \leqslant r \leqslant n$ and the following conditions at the interfaces $\Gamma_{(r-1,r)}$ hold true for $r = 2,\ldots,n$:

$$\left[\chi^{kl}_i\right] = 0 \tag{73}$$

and

$$\sigma_{ij}\left(\chi_{(pq)}\right)n_j = [C_{pqij}]|_{\Gamma_{(r-1,r)}}n_j = F_{(pq)i}|_{\Gamma_{(r-1,r)}} = C^{(r)}_{pqij} - C^{(r-1)}_{pqij}, \quad \mathbf{x} \in \Gamma_{(r-1,r)} \tag{74}$$

is a difference of the elasticity tensor values for the components Ω_{r-1} and Ω_r. Hence, the variational formulation necessary for the Finite Element Method analysis of the local problem can be written out as (see Kamiński and Schrefler, 2000)

$$\sum_{r=1}^{n}\int_{\Omega_r} C_{ijkl}\varepsilon_{kl}\left(\chi_{(pq)}\right)\varepsilon_{ij}(\mathbf{v}) = -\sum_{r=2}^{n}\int_{\Gamma_{(r-1,r)}} \sigma_{ij}(\chi_{(pq)})n_j v_i \,\mathrm{d}\Gamma + \int_{\Omega} f_i v_i \,\mathrm{d}\Omega. \tag{75}$$

Introducing definition (74) and neglecting composite body forces, it is obtained that

$$\sum_{r=1}^{n}\int_{\Omega_r} C_{ijkl}\varepsilon_{kl}\left(\chi^{(pq)}\right)\varepsilon_{ij}(\mathbf{v})\,\mathrm{d}\Omega = -\sum_{r=2}^{n}\int_{\Gamma_{(r-1,r)}} [C_{ijpq}]|_{\Gamma_{(r-1,r)}} n_j v_i \,\mathrm{d}\Gamma. \tag{76}$$

Further, the effective elasticity tensor components are derived from the following relation:

$$-\sum_{r=2}^{n}\int_{\Gamma_{(r-1,r)}} [C_{ijpq}]|_{\Gamma_{(r-1,r)}} n_j v_i \,\mathrm{d}\Gamma = \int_{\Omega} C_{ijpq}\varepsilon_{ij}(\mathbf{v})\,\mathrm{d}\Omega \tag{77}$$

to arrive at

$$\sum_{r=1}^{n}\int_{\Omega_r} C_{ijkl}\varepsilon_{kl}\left(\chi^{(pq)}\right)\varepsilon_{ij}(\mathbf{v})\,\mathrm{d}\Omega = \int_{\Omega} C_{ijkl}\varepsilon_{kl}\left(\chi^{(pq)}\right)\varepsilon_{ij}(\mathbf{v})\,\mathrm{d}\Omega = -\int_{\Omega} C_{ijpq}\varepsilon_{ij}(\mathbf{v})\,\mathrm{d}\Omega. \tag{78}$$

Therefore, it yields

$$C_{ijpq}^{(\mathrm{eff})} = \frac{1}{|\,\Omega\,|}\int_{\Omega}\left(C_{ijpq} + C_{ijkl}\varepsilon_{kl}\left(\boldsymbol{\chi}^{(pq)}\right)\right)\mathrm{d}\Omega. \tag{79}$$

Summing up all the considerations dealing with the homogenization problem, the effective elasticity tensor components are computed using Eq. (79) thanks to the homogenization function $\chi_{(kl)i}$ being a solution to a boundary value problem with periodicity conditions on external boundaries of Ω; the stress boundary conditions are equal to the difference of constitutive tensor components at the composite interface (see Eq. (74)).

It should be mentioned that the presented homogenization method has a general character due to the fact that the effective elasticity tensor components do not depend neither on the total number of composite components within the RVE nor on their shape, opposite to some previous models.

Further, analyzing Eq. (79), it is clear that if the second component of the R.H.S. integrand function is omitted, well-known upper bounds for the effective elasticity tensor for the composite are returned (Christensen, 1979; Milton, 2002). The experimental and computational analyses prove that these bounds are easy to calculate even for the case of random spaces of composite constituents elastic characteristics, but their values are significantly exaggerated in comparison to the real effective properties. To reduce these bounds, the local problem described above is solved and the displacement homogenization function components are computed.

3. Computational implementation

Let us introduce the following approximation of homogenization functions $\chi_{(uv)i}$ at any point of the considered continuum Ω in terms of a finite number of generalized coordinates $q_{(uv)\alpha}$ and shape functions $\varphi_{i\alpha}$:

$$\chi_{(uv)i} = \varphi_{i\alpha} q_{(uv)\alpha}, \quad i,u,v = 1,2, \;\; \alpha = 1,\ldots,N \tag{80}$$

and the strain $\varepsilon_{ij}(\chi_{(uv)})$ as well as stress $\sigma_{ij}(\chi_{(uv)})$ tensors

$$\varepsilon_{ij}\left(\chi_{(uv)}\right) = B_{ij\alpha}q_{(uv)\alpha}, \tag{81}$$

$$\sigma_{ij(uv)} = \sigma_{ij}\left(\chi_{(uv)}\right) = C_{ijkl}\varepsilon_{kl}\left(\chi_{(uv)}\right) = C_{ijkl}B_{kl\alpha}q_{(uv)\alpha}, \tag{82}$$

where $B_{kl\alpha}$ is a conventional FEM strain-nodal displacement operator and the virtual work equation looks like

$$\int_{\Omega}\delta\chi_{(uv)i,j}C_{ijkl}\chi_{(uv)k,l}\,\mathrm{d}\Omega = \sum_{r=2}^{n}\int_{\Gamma_{(r-1,r)}}\delta\chi_{(uv)i}[F_{(uv)i}]|_{\Gamma_{(r-1,r)}}\,\mathrm{d}\Gamma \quad (\text{no sum on } u,v). \tag{83}$$

Next, let us define the global stiffness matrix as

$$K_{\alpha\beta} = \sum_{e=1}^{E}K_{\alpha\beta}^{(e)} = \sum_{e=1}^{E}\int_{\Omega_e}C_{ijkl}^{(e)}B_{ij\alpha}B_{kl\beta}\,\mathrm{d}\Omega. \tag{84}$$

Introducing this matrix into Eq. (83) and minimizing it with respect to the generalized coordinates we arrive at

$$K_{\alpha\beta}q_{(uv)\alpha} = Q_{(uv)\alpha}, \tag{85}$$

where the R.H.S. vector consists of the stress interface conditions. To assure the symmetry conditions on the periodicity cell quarter, the orthogonal displacements and rotations for every nodal point belonging to the external boundaries of Ω are fixed. For the functions $\chi_{(uv)i}$ so obtained, we compute the resulting stresses and then average them numerically over the region Ω.

In the case of randomly varying elastic characteristics of the composite, probabilistic moments of the effective elasticity tensor are computed. Expected values of the tensor can be determined as follows:

$$E\left[C_{ijpq}^{(\mathrm{eff})}\right] = E\left[\langle C_{ijpq}\rangle_{\Omega}\right] + E\left[\left\langle C_{ijkl}\varepsilon_{kl}\left(\chi_{(pq)}\right)\right\rangle_{\Omega}\right], \tag{86}$$

while the variances have the form

$$\mathrm{Var}\left(C_{ijpq}^{(\mathrm{eff})}\right) = \mathrm{Var}\left(\langle C_{ijpq}\rangle_{\Omega}\right) + \mathrm{Var}\left(\left\langle C_{ijkl}\varepsilon_{kl}\left(\chi_{(pq)}\right)\right\rangle_{\Omega}\right) + 2\mathrm{Cov}\left(\langle C_{ijpq}\rangle_{\Omega};\left\langle C_{ijkl}\varepsilon_{kl}\left(\chi_{(pq)}\right)\right\rangle_{\Omega}\right). \tag{87}$$

Probabilistic moments of the effective characteristics are determined using Monte-Carlo simulation technique and the statistical estimation methods (Bendat and Piersol, 1971; Boswell et al., 1993) thanks to the unbiased estimators of effective elasticity tensor components. Finally, the following limits for Gaussian variables:

$$\lim_{M\to\infty}\beta\left(C_{ijkl}^{(\mathrm{eff})}\right) = 0, \quad \lim_{M\to\infty}\gamma\left(C_{ijkl}^{(\mathrm{eff})}\right) = 3 \tag{88}$$

are employed. They are very useful together with the PDF estimator to verify the output probabilistic distribution functions type, which is completely impossible by theoretical derivations.

4. Numerical experiments

4.1. Symbolic computations of interphase material parameters

The first group of numerical experiments deals with symbolic computations of the homogenized parameters for the interphase using the mathematical package MAPLE V (see Cornil and Testud, 2001). Using basic equations derived in Section 2.3 together with the perturbation analysis implemented in this program, probabilistic moments for the effective Young modulus and Poisson ratio are computed. Taking into account the limitations on input random variations in the perturbation analysis, 2nd, 4th, 6th, 8th and

10th order equations have been derived symbolically to eliminate those limitations. Effective interphase parameters are determined in the case of the fiber-reinforced composite, where all the semi-elliptical defects are located in the matrix around the fiber-matrix interface. The following data are inserted into the MAPLE script: $R = 0.5$ (fiber radius), $E[e_m] = 4.0\,\mathrm{GPa}$, $\sigma(e_m) = 0.0\,\mathrm{GPa}$, $\nu_m = 0.34$, $E[a] = 0.005$; standard deviations for all geometrical input random quantities are assumed to be at the level of 15% of the relevant expected values. Young modulus of the matrix is practically adopted as a deterministic parameter to separate the influence of its randomness from random fluctuations of the defects. Visualization tools of the program are engaged to demonstrate the variability of expectations for homogenized interphase elastic parameters with respect to (1) the flatness parameter relating expected values of minor to major semi-axes of the defects as well as to (2) expected value of the defects number. The maximal value of this parameter equal to 100 corresponds to the situation, where the defects occupy about 33% of the entire fiber-matrix boundary.

As it can be seen from comparison of Figs. 5 and 6 with Figs. 7 and 8, the differences between 2nd and 10th order results can be neglected for the randomness input level chosen, however these differences can change together with increasing standard deviations of defects parameters. Some verification of

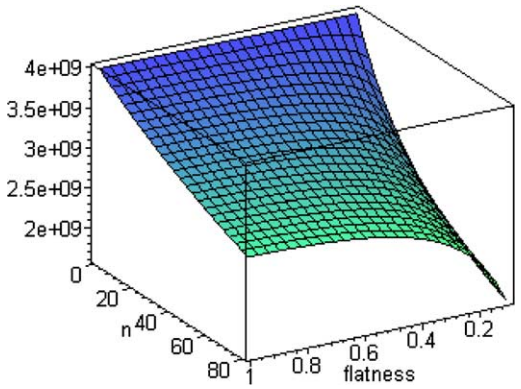

Fig. 5. Expected values for homogenized Young modulus, 2nd order perturbation approach.

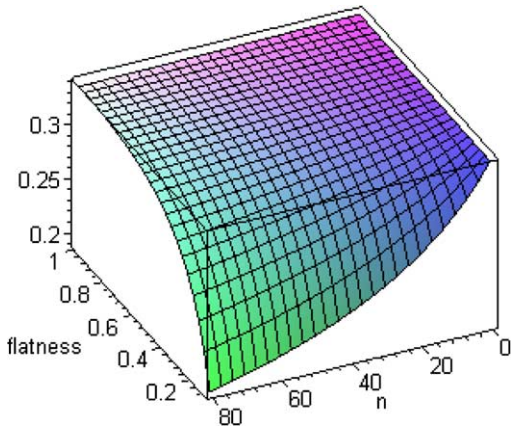

Fig. 6. Expected values for homogenized Poisson ratio, 2nd order perturbation approach.

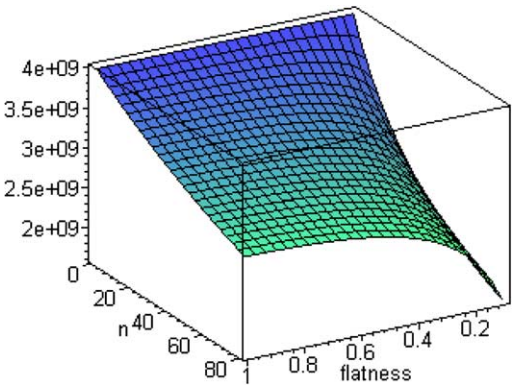

Fig. 7. Expected values for homogenized Young modulus, 10th order perturbation approach.

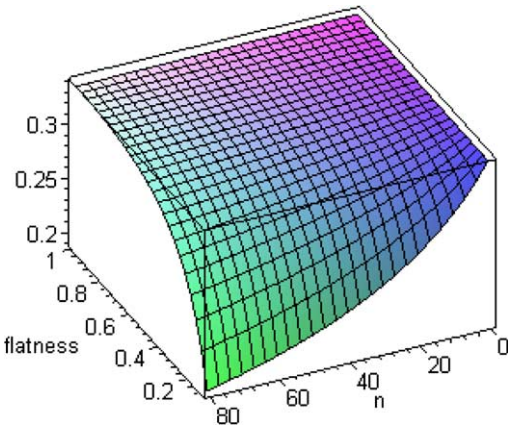

Fig. 8. Expected values for homogenized Poisson ratio, 10th order perturbation approach.

homogenized formulas is obtained for $E[n] = 0$, where the initial elastic parameters for the matrix are obtained. The greatest decrease of effective elastic parameters for interphase is obtained for lower limit on the flatness parameters. It means that the worst scenario for the composite is to introduce long cracks between the matrix and the fiber along the interface; then the expected values of interphase Young modulus and Poisson ratio decrease more than twice. The smallest decrease of these homogenized parameters is obtained in the case when the flatness parameter is equal to 1, which is equivalent to semi-circular interface defects; Young modulus decreases for more than 25% of its initial value, whereas the Poisson ratio is almost non-sensitive to any changes.

Standard deviations of the homogenized Young modulus and Poisson ratio for the interphase are collected in Figs. 9 and 10, correspondingly. They are obviously equal to 0 when the total number of the defects equals to 0, quite similarly to the relevant expected values. As it is documented in Fig. 10, the Poisson ratio standard deviations are also equal to 0 for unitary flatness parameter and for any number of the defects along the interface. Further, the greatest decrease is observed once more in the case of the flatness parameter minimum for both effective Young modulus and Poisson ratio; generally standard deviations do not exceed the input variables standard deviations level.

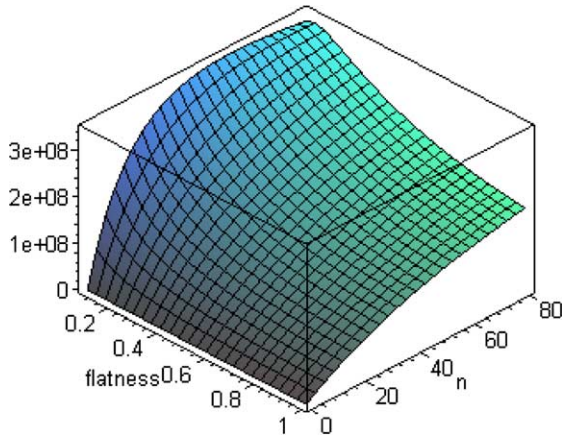

Fig. 9. Standard deviations for homogenized Young modulus, 2nd order perturbation approach.

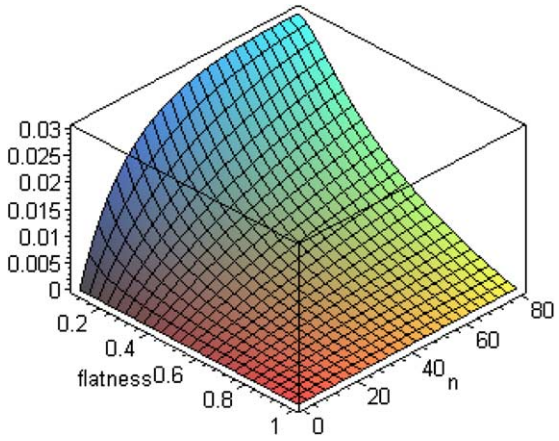

Fig. 10. Standard deviations for homogenized Poisson ratio, 2nd order perturbation approach.

4.2. Probabilistic analysis of the homogenized elasticity tensor

A numerical analysis of the periodic random fiber composite homogenization with stochastic interface defects is performed using the specially adopted FEM and homogenization-oriented program MCCEFF (Kamiński, 1995). Internal automatic generator of this program for the square RVE with centrally located round fiber occupying 50% of the RVE with interface defects is used to prepare the mesh; discretization with 144 four-noded plane strain finite elements and 153 nodes is displayed in Fig. 11.

Considering the greater composite sensitivity to the matrix defects, only a fiber-reinforced structure with such voids is analyzed. Elastic parameters of the fiber material are taken as $E[e_1] = 84\,\mathrm{GPa}$, $\nu_1 = 0.22$ and for the matrix $E[e_2] = 4\,\mathrm{GPa}$, $\nu_2 = 0.34$, while standard deviations for both Young moduli are equal to 0.15 of the corresponding expectations. 3.000 Monte-Carlo samples are performed each time for a flatness parameter of the defects equal to 1.5 ($E[b] = 0.010$ and $E[a] = 0.015$) and expectations of their total number equivalent to 0%, 12%, 24%, 36% and 48% ($E[n] = 0$, 10, 20, 30, 40 and 50) of the entire fiber-matrix interface length. All the input and output data are collected in Table 1. For a specific value of $E[n]$, the expected

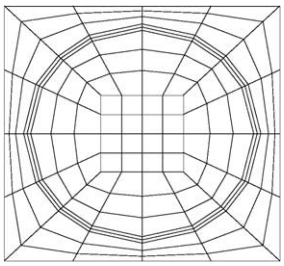

Fig. 11. FEM discretization of periodicity cell.

Table 1
Input and output data in FEM homogenization

$E[n]$	$E[e^{(\mathrm{eff})}]$	$v^{(\mathrm{eff})}$	$\mathrm{Var}(e^{(\mathrm{eff})})$	$C_{1111}^{(\mathrm{eff})}$	$C_{1122}^{(\mathrm{eff})}$	$C_{1212}^{(\mathrm{eff})}$
0	4.0000E9	0.3400	0.3600E18	15.342	5.0928	17.587
				0.15235	0.15235	0.15235
				0.027063	0.027109	0.027101
				3.101	3.1013	3.1014
10	3.3236E9	0.3348	0.2683E18	15.036	5.0344	17.578
				0.15299	0.15265	0.15236
				0.026992	0.027041	0.027097
				3.1013	3.1015	3.1014
20	2.8487E9	0.3313	0.2234E18	14.755	4.9816	17.571
				0.15434	0.15332	0.15239
				0.025878	0.026366	0.027132
				3.1028	3.1021	3.1014
30	2.4955E9	0.3287	0.1931E18	14.492	4.9319	17.566
				0.15598	0.15417	0.15240
				0.023015	0.024824	0.027095
				3.1057	3.1040	3.1014
40	2.2216E9	0.3267	0.1693E18	14.245	4.8843	17.562
				0.15775	0.15515	0.15241
				0.019253	0.021971	0.027103
				3.1103	3.1077	3.1013
50	2.0028E9	0.3252	0.1497E18	14.011	4.8381	17.559
				0.15953	0.15620	0.15242
				0.014316	0.018409	0.027108
				3.1171	3.1125	3.1013

values and variances of interphase effective Young modulus and Poisson ratio are given together with (1) expected values, (2) coefficients of variation, (3) coefficients of asymmetry as well as (4) coefficients of flatness for the effective elasticity tensor components.

The first, most general observation is that all the analyzed random variables, in the context of Eq. (88), are with a good approximation Gaussian random variables. It eliminates the necessity of statistical estimation for higher than the second probabilistic moments. They can be recovered using a relevant integration of probability density function with expectations and standard deviations inserted from this initial Monte-Carlo based FEM estimation. This result was obtained before for the fiber-reinforced composites with

perfect interface as well as with semi-circular defects combined with interphase model (Kamiński, 1995). Constitutive relations for the interphase were essentially different and were based on a simple probabilistic version of the spatial averaging.

Furthermore, as it can be expected, an increase of the interface defects number decreases expectations for all the components of the effective elasticity tensor; the decreases collected in Table 1 are small, however essentially greater than those obtained before for the semi-circular interface defects and their spatial averaging into the interphase. It should be mentioned that this effect strongly depends on the defects flatness parameter – more essential changes should be observed for decreasing value of this parameter according to the results presented in Figs. 5–8. Those expectations decreases are the most apparent in the case of $C_{1111}^{(\mathrm{eff})}$; a quite similar relation is obtained for the asymmetry coefficients that are all positive. The only exception is $C_{1212}^{(\mathrm{eff})}$, where these coefficients oscillate around some value. Essentially different observations can be made in terms of coefficients of variation, whose values systematically increase together with $E[n]$, once more at most for the component $C_{1111}^{(\mathrm{eff})}$. The fourth order coefficients of flatness behave analogously, increasing their values above the value proposed by Eq. (88) for the Gaussian variables. It means that they are more concentrated around their expected values than it is obtained for composite structures with perfect interfaces.

Finally, the effective properties values collected in Table 1 do not change a lot from their initial values for the non-defected composite. However, they are obtained for small defects in comparison with the fiber radius. Their geometrical flatness parameter is adequate rather to porosity effects than to the interface cracks. This situation may essentially change if the defects shape tends to an elongated semi-ellipse, which should be the subject of further extended computational studies. Another interesting result can be obtained when the homogenized constitutive law will be implemented according to the assumption about the interacting interface defects, being a starting point to delamination modeling using the homogenization approach.

5. Concluding remarks

1. The multiscale homogenization method presented here makes it possible to estimate probabilistic moments for the effective elasticity tensor in the case of multicomponent composites with semi-elliptical interface defects. Such a model of the defects is relevant to both interface cracks (for greater flatness ratio between minor and major semi-axes of semi-ellipses) and natural matrix porosity or cavitation erosion (in the case of semi-circular voids between the components). As it is computed symbolically using the program MAPLE, probabilistic moments of effective interphase parameters are most sensitive to the defects total number at the interface in the case of a geometrical flatness parameter tending to 0. The greatest decrease of effective material parameters is obtained for the lower limit on this variable. It is consistent with the engineering observations that the cracks along the interfaces are most dangerous defects for composite behavior, whereas the semicircular defects do not modify the stresses around the fiber-matrix boundary to a significant extent.
2. As it is seen in the homogenization results, the effective elastic parameters on the microscale appear to be with a good accuracy Gaussian random variables for the new defects shape, which eliminates the necessity of higher than the second order probabilistic moment estimation and where essentially longer Monte-Carlo sample is necessary (Kamiński and Kleiber, 2000). A computational symbolic-FEM homogenization approach can be used to model effective properties for superconducting and/or reinforced concrete periodic composites. Finally, this methodology can be enriched with (a) thermomechanical multiscale analyses using algebraic results contained in (Christensen, 1979; Kalamkarov and Kolpakov, 1997; Milton, 2002), (b) image analysis programs and concepts (Terada et al., 1997) as well as (c) computational parallelization procedures (Cruz and Patera, 1995) to speed up the entire simulation process.

References

Bendat, J.S., Piersol, A.G., 1971. Random Data: Analysis and Measurement Procedures. Wiley, New York.

Bensoussan, A., Lions, J.L., Papanicolaou, G., 1978. Asymptotic Analysis for Periodic Structures. North-Holland, Amsterdam.

Boswell, M.T., et al., 1993. The art of computer generation of random variables. In: Rao, C.R. (Ed.), Handbook of Statistics, Computational Statistics, vol. 9. Elsevier.

Brandt, A.M., 1995. Cement-based Composites. Materials, Mechanical Properties and Performance. Chapmann & Hall.

Christensen, R.M., 1979. Mechanics of Composite Materials. Wiley, New York.

Cornil, J.M., Testud, P., 2001. An Introduction to Maple V. Springer-Verlag, Berlin, Heidelberg.

Cruz, M.E., Patera, A.T., 1995. A parallel Monte-Carlo finite element procedure for the analysis of multicomponent media. International Journal for Numerical Methods in Engineering 38, 1087–1121.

Feller, W., 1965. An Introduction to Probability Theory and Its Applications. Wiley, New York.

Ghosh, S., Lee, K., Moorthy, S., 1995. Multiple scale analysis of heterogeneous elastic structures using homogenization theory and Voronoi cell finite element method. International Journal of Solids and Structures 32, 27–62.

Golansky, D., Terada, K., Kikuchi, N., 1997. Macro and micro scale modeling of thermal residual stresses in metal matrix composite surface layers by the homogenization method. Computational Mechanics 19, 188–202.

Hammond, D.A., Amateau, M.F., Quenney, R.A., 1993. Cavitation erosion performance of fiber reinforced composites. International Journal of Composite Materials 27, 1522–1544.

Hurtado, J.E., Barbat, A.H., 1998. Monte Carlo techniques in computational stochastic mechanics. Archives in Computer Methods in Engineering 5 (1), 3–30.

Jasiuk, I., Chen, J., Thorpe, M.F., 1994. Elastic moduli of two-dimensional materials with polygonal and elliptical holes. In: Ostoja-Starzewski, M., Jasiuk, I. et al. (Eds.), Micromechanics of random media. Applied Mechanics Review ASME 47(1), pp. 18–28.

Jeulin, D., Ostoja-Starzewski, M. (Eds.), 2001. Mechanics of Random and Multiscale Structures. CISM Courses and Lectures No. 430, Springer, Wien, New York.

Kalamkarov, A.L., Kolpakov, A.G., 1997. Analysis, Design and Optimization of Composite Structures. Wiley.

Kamiński, M., 1995. Stochastic contact effects in periodic fibre composites. Journal of Theoretical and Applied Mechanics 2, 415–441.

Kamiński, M., Kleiber, M., 2000. Numerical homogenization of *n*-component composites including stochastic interface defects. International Journal for Numerical Methods in Engineering 47, 1001–1027.

Kamiński, M., Schrefler, B.A., 2000. Probabilistic effective characteristics of cables for superconducting coils. Computer Methods in Applied Mechanics and Engineering 188 (1–3), 1–16.

Lené, F., Leguillon, D., 1982. Homogenized constitutive law for a partially cohesive composite material. International Journal of Solids and Structures 18, 443–458.

Leo, P.H., Hu, J., 1995. A continuum description of partially coherent interfaces. Continuum Mechanics and Thermodynamics 7, 39–56.

Litewka, A., 1985. Effective material constants for orthotropically damaged elastic solid. Archives of Mechanics 37, 631–642.

Milton, G.W., 2002. The Theory of Composites. Cambridge University Press.

Mital, S.K., Murthy, P.L.N., Chamis, C.C., 1993. Interfacial microfracture in high temperature metal matrix composites. International Journal for Composite Materials 27, 1678–1694.

Pedersen, P. (Ed.), 1993. Optimal Design with Advanced Materials. Elsevier.

Sab, K., 1992. On the homogenization and the simulation of random materials. European Journal Mechanics Solids/A 11, 585–607.

Sanchez-Palencia, E., 1980. Non-Homogeneous Media and Vibration Theory. Springer-Verlag.

Schellekens, J.C.J., de Borst, R., 1994. The application of interface elements and enriched or rate-dependent continua to micro-mechanical analyses of fracture in composites. Computational Mechanics 14, 68–83.

Terada, K., Miura, T., Kikuchi, N., 1997. Digital image-based modeling applied to the homogenization analysis of composite materials. Computational Mechanics 20, 331–346.

Tsukrov, I., Kachanov, M., 2000. Effective moduli of an anisotropic material with elliptical holes of arbitrary orientational distribution. International Journal of Solids and Structures 37, 5919–5941.

Zavarise, G., Wriggers, P., Stein, E., Schrefler, B.A., 1992. Real contact mechanisms and finite element formulation—a coupled thermomechanical approach. International Journal for Numerical Methods in Engineering 35, 767–785.